ACTA NEUROBIOLOGIAE EXPERIMENTALIS

Acta Neurobiol. Exp. 1995, 55: 193-200

Topography of primary afferent projections in the trigeminal sensory nuclei of rats

Sherre L. Florence and **Shankar Lakshman**

Department of Psychology, 301 Wilson Hall, Vanderbilt University, Nashville, TN 37240, USA

Abstract. The afferent projection pattern from individual vibrissae follicles was related to the distribution of cytochrome oxidase (CO) dark cell clusters in the trigeminal sensory nuclei of adult rats to determine whether segregated primary afferent projections limit the extent of the topographic reorganizations that can occur at the level of the brainstem on a short term basis after changes in sensory driven activity. The results indicate that the projections to all the brain stem trigeminal subnuclei, including the principal sensory nucleus and the three subdivisions of the spinal trigeminal nucleus, are topographic; however, the extent to which label from different whisker rows overlap appears to differ from subdivision to subdivision. In the principal sensory nucleus there is nearly a one to one relationship between the inputs from the vibrissae follicles and the corresponding CO-dense clusters. Thus, little overlap of inputs from different vibrissae rows is likely. In contrast, in the pars interpolaris and, to a lesser extent, in the pars caudalis, inputs from individual vibrissae follicles extend beyond the appropriate CO-dark patch into adjacent whisker patches; thus, inputs to these subdivisions from different vibrissae likely overlap more extensively.

Short communication

Key words: vibrissae, dorsal column nuclei, primary afferents, transganglionic transport, rodents

The highly ordered, topographic relationship between sensory receptors in the periphery and target neurones in the brain is best characterized by the rodent whisker barrel system. Histochemical staining techniques have revealed patterns of darkly staining cell and axon clusters which replicate the arrangement of vibrissae on the face throughout the somatosensory pathway. At each level of the pathway, a single vibrissa is represented by a cell cluster that stains darkly for histochemical markers such as cytochrome oxidase or succinic dehydrogenase (brain stem - Belford and Killackey 1979, Durham and Woolsey 1984, Ma and Woolsey 1984: thalamus - Van der Loos 1976, Belford and Killackey 1982, Ivy and Killackey 1982: cortex - Woolsey and Van der Loos 1970). When one or more of the vibrissae are destroyed during early stages of development or when the infraorbital nerve, which innervates the vibrissae, is cut, the pattern of clustered cells changes so as to reflect, in a one-to-one fashion, the altered vibrissa pattern on the face (e.g. Van der Loos and Woolsey 1973, Belford and Killackey 1979, Woolsey et al. 1979, Bates et al. 1982, Durham and Woolsey 1984, Bates and Killackey 1985, Chiaia et al. 1992).

Afferent input patterns also replicate the distribution of the vibrissae, both in normal animals and after early vibrissae removal or infraorbital nerve cut, at all levels of the somatosensory pathway, including: the trigeminal sensory nuclei (e.g. Bates and Killackey 1985, Jacquin and Rhoades 1985, Rhoades et al. 1989, Takemura et al. 1991, Chiaia et al. 1992), the ventrobasal complex (e.g. Belford and Killackey 1982, Ivy and Killackey 1982), and the primary somatosensory cortex (e.g. Killackey 1973, Van der Loos and Woolsey 1973, Killackey et al. 1976). Morphological analysis of individual axons indicates that afferents activated by a specific vibrissa tend to have very circumscribed projections (e.g. Hayashi et al. 1985, Jacquin et al. 1986a,b, 1993b), and at least in the principal sensory nucleus, projections are restricted largely to the appropriate whisker-related patch (Jacquin et al. 1993b). However, these studies typically involve assessments of only a small number of the overall population of inputs. Thus, it remains unclear whether there is indeed a 1:1 relationship between the peripheral afferents from individual vibrissae follicles and vibrissae-related cell clusters. An assessment of the precision of primary sensory projections to specific cell clusters at this early level in the central nervous system might indicate the limits of change that are possible in response to injury, learning and experience at early stages of the processing hierarchy.

The approach in the present study was to use the transganglionic tracing technique to label the afferent projection patterns from one or more whisker follicles, and then to relate the label to the cytochrome oxidase (CO) staining patterns of the trigeminal nuclei in adult rats. The procedures have been described in detail elsewhere (see Florence et al. 1989, 1991). Briefly, small (2-7 μl) subcutaneous injections of 0.1-1.0% cholera toxin subunit B bound to horseradish peroxidase (BHRP) were made either below or directly into whisker follicles of 6 adult rats (Sprague-Dawley) anaesthetized with ketamine hydrochloride (90 mg/kg, IM) supplemented with xylazine (16 mg/kg, IM). The number and size of the injections varied. In some animals, single 2-3 μl injections were made with a Hamilton syringe equipped with a 30 gauge needle into an identified whisker follicle of vibrissae row A, C or E. For these restricted injections the whisker was first removed with forceps, and the needle was inserted directly into the follicle. In other animals, larger (5-7 μl) injections were made at multiple sites subcutaneously along a row of whiskers. In most cases, injections were made on both sides of the face, since this technique has been shown to label only ipsilateral projections (e.g. Arvidsson 1982). After a 3-5 day survival period, the rats were given a lethal dose of sodium pentobarbital (IP) and perfused through the heart with a rinse of 0.9% saline followed by a fixative of 2-4% paraformaldehyde. The brain stems were stored overnight in 30% sucrose in phosphate buffer (pH 7.4) and then frozen sectioned in the coronal plane on a sliding microtome. Alternate series of sections were processed either with tetramethyl benzedine (TMB) to vis-

ualize the HRP conjugate, or with CO to reveal the structural parcellation patterns. Drawings of labelled TMB sections were made using a microscope equipped with a drawing tube. Then, nuclear borders and parcellation patterns were added to the drawings by projecting adjacent CO-reacted sections on the drawing of the TMB sections using common blood vessels and tissue artifacts for alignment.

All portions of the trigeminal brain stem nucleus stain darkly for CO. Subdivisions related to the whisker pattern on the face generally are not as distinct in the adult as they are in young rats (e.g. Belford and Killackey 1979). However, in the trigeminal subnuclei where whisker related patterns have been demonstrated previously (principal sensory nucleus, pars interpolaris, pars caudalis) CO-dark regions separated by CO-light gaps were apparent. The CO staining patterns in each subnucleus will be described separately below.

The injections resulted in anterograde labelling in the principal sensory nucleus, and in the three subdivisions of the spinal trigeminal nucleus. In general, the projections to all the subdivisions were in topographic register, so that injections of the more dorsally situated whisker follicles (i.e. those in row A) labelled the ventral portions of the trigeminal nuclei, and injections of ventral follicles resulted in more dorsally situated label. Small injections resulted in punctate projections in some parts of the trigeminal nuclei, and in other subnuclei the label was more disperse. Thus, although no attempt was made to define the extent of the spread from the injection, comparisons across levels of the trigeminal brain stem nuclei reveal differences in topographic precision of inputs. Injections often labelled cell bodies in the nucleus of the facial nerve (VII); these data will not be discussed further. Label in other traditionally "non-trigeminal" areas that are known to receive inputs from the trigeminal nerve (e.g. Jacquin et al. 1982, Pfaller and Arvidsson 1988, Marfurt and Rajchert 1991) was not found, presumably because in the present study the injections labelled only a small fraction of the total trigeminal nerve inputs.

In the principal sensory nucleus (PSN), CO staining was relatively dense. In the ventral half of PSN, the CO-dark clusters related to the vibrissae were separated by CO-light gaps (Fig. 1A). In the dorsal portion of the nucleus, CO-light zones subdivided the nucleus in an irregular, fractured pattern (Fig. 1A). Injections of single vibrissae labelled discrete zones in the ventral portion of the nucleus. The terminals formed a small focus of very dense label, with scattered label extending in the surrounding neuropil (Fig. 1B). Compared to the size of labelled regions in other trigeminal nuclei, the total labelled extent was quite restricted. Typically, the densest portion of label was concentrated in a single CO--dense band, with lighter label extending into adjacent CO-dense bands (Fig. 1); the band in which the label was most concentrated was appropriate for the follicle injected. For example, injections into one or more follicles in vibrissae row A label the extreme ventral CO-dense band; injections in row C, label a more dorsal CO-dense band, and injections in row E label the most dorsal of these prominent CO-dense bands. As would be expected, large or multiple injections involving more that one vibrissae row resulted in PSN labelling across multiple CO-dense bands (Fig. 3). In contrast, multiple injections within the same row of whisker follicles resulted in projections equally as restricted in the coronal plane as projections from a single follicle, although rostrocaudally the label was more extensive.

The CO staining pattern in the pars oralis (OR) is relatively light, and reticulations within OR obscure the variations in CO density related to topography (Fig. 1C). After injections of the vibrissae label in OR was very sparse (Fig. 1D), nonetheless the topography of the projections was evident. For example, a restricted injection in the A row resulted in diffuse label ventral in OR and injections involving rows B and C labelled progressively more dorsal portions of the nucleus (Fig. 3). Multiple injections resulted in more widespread labelling than single small injections.

The CO staining pattern in the pars interpolaris (INT) is moderate, and despite the numerous reticulations within INT, there are distinct CO-light bands

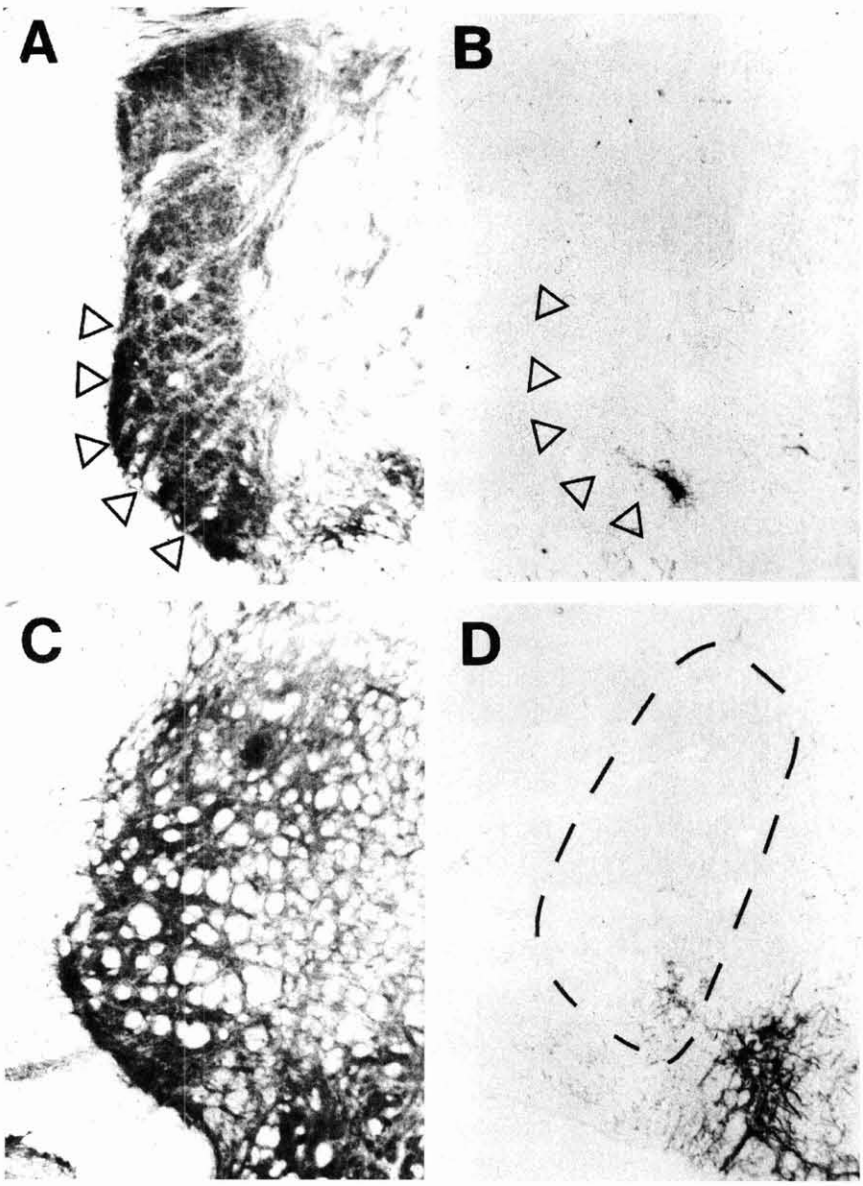

Fig. 1. Demonstration of the relationship between labelled projections from the A4 vibrissa follicle and the CO staining patterns in the principal sensory nucleus (PSN) and pars oralis (OR) of rats. A, the CO staining pattern in a frontal section through PSN. Arrowheads indicate CO-light gaps that separate CO-dense regions related to rows of mystacial whiskers. B, photomicrograph of the distribution of label after a 3 µl injection of cholera toxin subunit B conjugated to HRP into the A4 vibrissa follicle showing the distribution of label from a section adjacent to the one shown in A. A small, dense focus of label is situated in the CO-dark band that corresponds to the A row of vibrissae follicles, and only faint label extends into the CO--dense bands related to the adjacent whisker row. In order to relate the label to the whisker related CO patches in A, arrowheads indicate approximate locations of the CO-light gaps in adjacent CO sections. Dorsal is to the top and medial is to the right. C, CO staining pattern in a frontal section through OR. D, photomicrograph of the distribution of label in OR after the injection (described above) into whisker follicle A4. Dashed line indicates the borders of OR. Densely labelled cell bodies ventromedial to OR are in the facial nucleus.

separating the CO-dark clusters related to the vibrissae (Fig. 2A). The label typically was more dense than in the OR but much more sparse than in CAUD (Fig. 2B), and while the projections appear to be topographic, they are not as precise as in PSN. For example, although the majority of label was restricted to the appropriate CO-dark patch after a small injection of the A4 follicle, a second focus of light label was located more dorsally in the region where inputs from follicles in the C row would be located (Fig. 2B). Multiple injections involving rows B and C resulted in a somewhat larger focus of label that spanned several CO subdivisions (Fig. 3).

In the pars caudalis (CAUD), CO staining is more intense than in any of the other trigeminal brain stem nuclei. CO-light gaps separating the CO--dark regions demarcating the vibrissae-related subdivisions are most prominent laterally in CAUD, through the marginal zone and substantia gelatinosa (Fig. 2C). The injections resulted in dense labelling in the substantial gelatinosa, where it is concentrated primarily in the appropriate CO--dense whisker related patch (Fig. 2D). Dense label typically extends a small distance into adjacent CO--dense bands (Fig. 2D). Comparison of the labelling patterns after injections of different whisker rows,

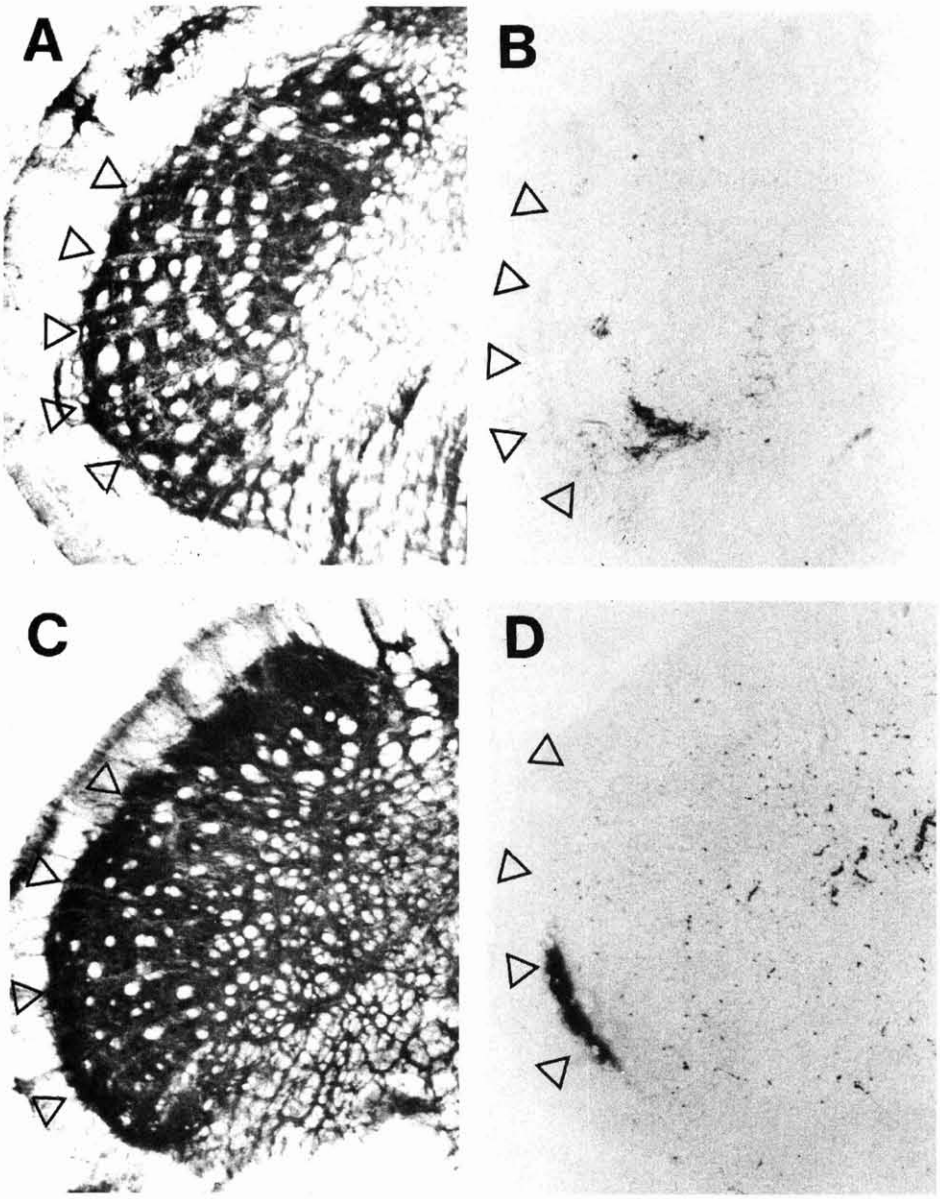

Fig. 2. Demonstration of the relationship between labelled projections from the A4 vibrissa follicle and the CO staining patterns in the pars interpolaris (INT) and pars caudalis (CAUD) of rats. A, the CO staining pattern in a frontal section through INT. Arrowheads indicate CO-light gaps that separate CO-dense regions related to rows of mystacial whiskers. B, photomicrograph of the distribution of label after a 3 µl injection of cholera toxin subunit B conjugated to HRP into the A4 vibrissa follicle showing the distribution of label from a section adjacent to the one shown in A. In order to relate the label to the CO staining pattern in A, arrowheads indicate approximate locations of the CO-light gaps in adjacent CO sections. Dorsal is to the top and medial is to the right. C, CO staining pattern in a frontal section through CAUD. D, photomicrograph of the distribution of label in the CAUD after the injection (described above) into whisker follicle A4. Arrowheads indicate approximate locations of the CO-light gaps separating CO dark whisker related patches.

demonstrates the topographic order to the projections. For example, an injection of whisker row A results in dense label in the ventral-most CO band (Fig. 2D), while an injection in the C row results in label concentrated in the third in a ventrodorsal series of CO-dense bands, and injections in the E row results in label in an even more dorsally-situated CO-dense band. Large or multiple injections involving more than one vibrissae row result in dense label of multiple CO-dense bands (Fig. 3). In addition to the dense labelling in the substantia gelatinosa, sparse label was found in the magnocellular layer after large or multiple injections. In these cases, the label extended more rostral in CAUD than the dense labelling in the substantia gelatinosa, but had a dorsoventral extent that was similar (Fig. 3).

The present findings demonstrate that projections from discrete regions of the whisker pad to all the trigeminal nuclei have topographic termination patterns. These findings are in good agreement with the reports of others using the same approach as in the present report to study the distribution of vibrissae afferents in rats (Arvidsson 1982, Robertson and Arvidsson 1985, Arvidsson and Rice 1991,

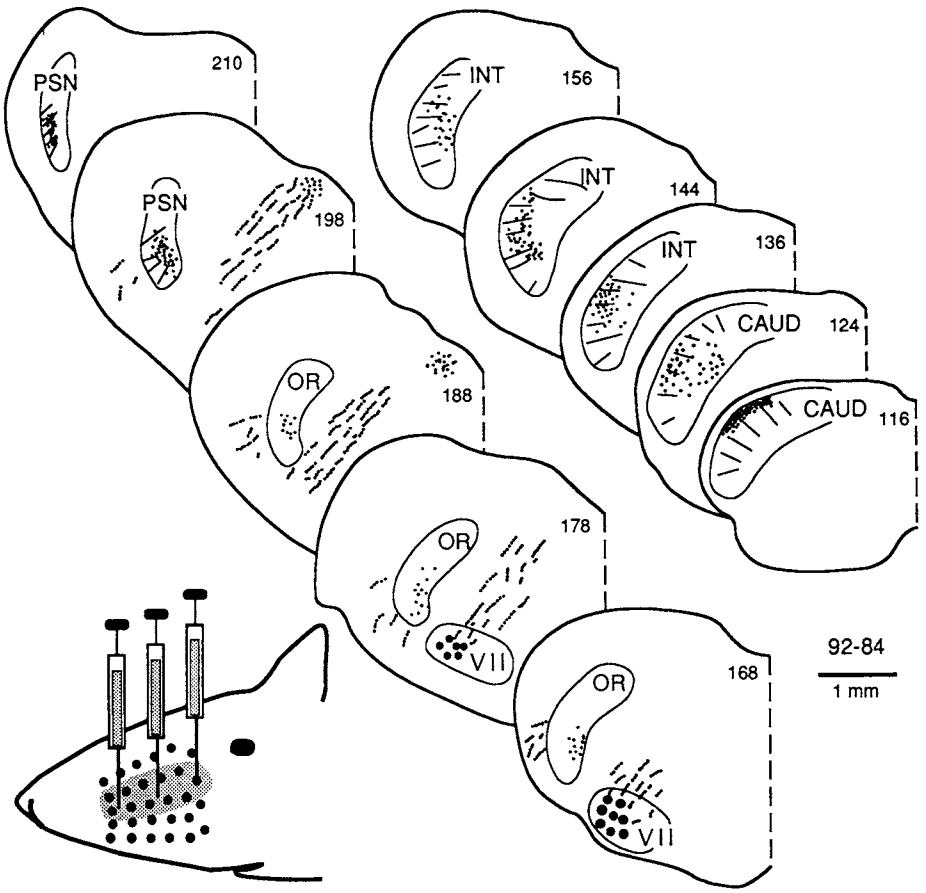

Fig. 3. Drawings of frontal sections through the trigeminal sensory nucleus in a rat after three injections of wheat germ agglutinin conjugated to HRP along the C row of vibrissae. The figurine shows the locations of the injections and approximate extent of the injection sites. Subdivisions within the trigeminal sensory nuclei are based on CO-stained sections adjacent to those reacted for the injected tracer. Labelling is indicated by the fine dots; label lateral to the trigeminal nuclei is from the trigeminal nerve, and label medial to the nuclei is from the facial nerve. Large dots depict label neurones in the facial nerve nucleus. The numbers indicate the position of the section in the series which progresses from caudal to rostral as the numbers go from low to high. Dorsal is to the top of each section and medial is to the right (midline is indicated by a dashed line). CAUD, pars caudalis; INT, pars interpolaris; OR, pars oralis, PSN, principal sensory nucleus; VII, facial nucleus.

Takemura et al. 1991). Other approaches such glucose utilization studies (2DG) (in mice - Melzer et al. 1985, 1994; in hamsters - Jacquin et al. 1993a) and morphological analyses of individual axons (e.g. Hayashi et al. 1985, Jacquin et al. 1986a,b, 1993b) also confirm the somatotopic nature of the projections.

Fewer studies have directly assessed the relationship between the afferent projections and the structural subdivisions related to the vibrissae. Our data indicate that, in the principal sensory nucleus, there is a nearly one to one relationship between the inputs from the vibrissae follicles and the corresponding CO-dense clusters. This result supports the findings of Jacquin et al. (1993b) in a study of the morphology of individual trigeminal afferent axons. They showed that in PSN axon collaterals were concentrated within the appropriate CO-dense subdivision, and terminal branches rarely crossed into adjacent, inappropriate CO-dense regions. A study of glucose (2DG) utilization in hamsters (Jacquin et al. 1993a) also indicates that the area of highest glucose utilization in PSN during stimulation of individual vibrissae corresponds with the CO-dense patch related to the stimulated whisker.

The relationship between the terminations of primary sensory afferents and whisker-related parcellations is less clear in the subdivisions of the spinal trigeminal nucleus. In the pars oralis, the topography of the inputs mimics that in the other trigeminal subdivisions, but we were unable to detect any topographic precision given that the whisker--related pattern is unapparent using structural markers such as CO. The sparsity of projections to OR demonstrated by the skin injection technique (present report; see also Arvidsson 1982, Robertson and Arvidsson 1985, Arvidsson and Rice 1991) likely explains the lack of evidence for 2DG uptake in OR after vibrissae stimulation (Melzer et al. 1985, 1994, Jacquin et al. 1993b). In the pars interpolaris,

although the projections are in topographic register, our data indicate that inputs to INT from individual vibrissae do not correlate directly with the vibrissae-related subdivisions. Thus, the topography is likely more crude in INT than in PSN. While no direct correlations have been made between the terminations of individual afferent axons and the whisker related subdivisions in INT; it appears that the terminations of individual axons from different vibrissae rows are not spaced widely enough to allow for non-overlapping representations of each whisker (Jacquin et al. 1993b). Individual axons have more punctate terminations in INT than would be expected from the relatively widespread label using the skin injection approach (e.g. Hayashi et al. 1985, Jacquin et al. 1986a,b, 1993b). This difference presumably demonstrates that analyses of individual axons do not indicate the full extent of variation in the afferent population whereas the skin injection approach, which presumably labels a large number of afferents including vibrissae and non-vibrissae inputs, reveals a somewhat more widespread terminal projection than individual axons. Studies of the pattern of 2DG uptake in hamsters indicates that after stimulation of individual whiskers, uptake is highest directly over the appropriate CO--dense whisker patch in INT (Jacquin et al. 1993a). This would indicate that there is nearly a 1:1 projection pattern from the whiskers to CO patches in INT, in apparent conflict with our data. However, the activity patterns revealed with the 2DG method will not reveal inputs that do not normally have significant functional impact. Presumably the sparse, off-focus projections shown in the present report are not normally activated to the same degree as the topographically appropriate inputs by the whisker stimulation paradigm used in the 2DG methods. Since changes in activity patterns can result in a strengthening of weak synaptic inputs (e.g. Bear et al. 1987) the off-focus projections may be at least partially responsible for topographic reorganizations in the somatosensory pathway after changes in the sensory environment. The projection from individual whisker follicles to CO-dense patches in CAUD is more precise than in either OR or INT, but the projection does not have the point to point precision that is present in PSN. These data support the finding of Jacquin et al. (1993b) who concluded from the study of the distribution of terminal arbors from individual axons that inputs to CAUD from vibrissae in adjacent whisker rows likely overlap somewhat, and are not as topographically precise as in PSN. In contrast, results from the study of 2DG uptake patterns after stimulation of individual vibrissae in hamsters indicates the uptake is topographically restricted in CAUD (Jacquin et al. 1993a); however, as discussed above this method does not reveal inputs with low levels of excitation, and thus the off-focus inputs demonstrated in the present report may reflect functionally ineffective inputs.

We are grateful to Judy Ives and Laura Trice for technical assistance. This work was supported by the John F. Kennedy Center for Research on Education and Human Development (NICHDHD15052).

Arvidsson J. (1982) Somatotopic organization of vibrissae afferents in the trigeminal sensory nuclei of the rat studied by transganglionic transport of HRP. J. Comp. Neurol. 211: 84-92.

Arvidsson J., Rice F.L. (1991) Central projections of primary sensory neurons innervating different parts of the vibrissae follicles and intervibrissal skin on the mystacial pad of the rat. J. Comp. Neurol. 309: 1-16.

Bates C.A., Erzurumlu R.S., Killackey H.P. (1982) Central correlates of peripheral pattern alterations in the trigeminal system of the rat. Dev. Brain Res. 5: 108-113.

Bates C.A., Killackey H.P. (1985) The organization of the neonatal rat's brainstem trigeminal complex and its role in the formation of central trigeminal patterns. J. Comp. Neurol. 240: 265-287.

Bear M.F., Cooper L.N., Ebner F.F. (1987) A physiological basis for a theory of synapse modification. Science 237: 42-48.

Belford G.R., Killackey H.P. (1979) Vibrissae representation in subcortical trigeminal centers of the neonatal rat. J. Comp. Neurol. 183: 305-322.

Belford G.R., Killackey H.P. (1982) Development of trigeminothalamic afferents to the ventrobasal complex of the neonatal rat. Anat. Rec. 202: 14a.

Chiaia N.L., Bennett-Clarke C.A. Rhoades R.W. (1991) Effects of cortical and thalamic lesions upon primary afferent terminations, distributions of projection neurons, and the

cytochrome oxidase pattern in the trigeminal brainstem complex. J. Comp. Neurol. 303: 600-616.

Chiaia N.L., Bennett-Clarke C.A., Rhoades R.W. (1992) Differential effects of peripheral damage on vibrissa-related patterns in trigeminal nucleus principalis, subnucleus interpolaris, and subnucleus caudalis. Neuroscience 49: 141-156.

Durham D., Woolsey T.A. (1984) Effects of neonatal whisker lesions on mouse central trigeminal pathways. J. Comp. Neurol. 223: 424-447.

Erzurumlu R.S., Ebner F.F. (1988) Maintenance of discrete somatosensory maps in subcortical relay nuclei is dependent on an intact sensory cortex. Dev. Brain Res. 44: 302-308.

Florence S.L., Wall J.T., Kaas J.H. (1989) Somatotopic organization of inputs from the hand of the spinal grey and cuneate nucleus of monkeys with observations on the cuneate nucleus of humans. J. Comp. Neurol. 286: 48-70.

Florence S.L., Wall J.T., Kaas J.H. (1991) Central projections from the skin of the hand in squirrel monkeys. J. Comp. Neurol. 311: 563-578.

Hayashi H. (1985) Morphology of central terminations of intra-axonally stained large, myelinated primary afferent fibers from facial skin in the rat. J. Comp. Neurol. 237: 195-215.

Ivy G.O., Killackey H.P. (1982) Ephemeral cellular segmentation in the thalamus of the neonatal rat. Dev. Brain Res. 2: 1-1.

Jacquin M.F., McCasland J.S., Henderson T.A., Rhoades R.W., Woolsey T.A. (1993a) 2-DG uptake patterns related to single vibrissae during exploratory behaviors in the hamster trigeminal system. J. Comp. Neurol. 332: 38-58.

Jacquin M.F., Renehan W.E., Mooney R.D., Rhoades R.W. (1986a) Structure-function relationships in rat medullary and cervical dorsal horns. I. Trigeminal primary afferents. J. Neurophysiol. 55: 1153-1186.

Jacquin M.F., Renehan W.E., Rhoades R.W., Panneton W.M. (1993b) Morphology and topography of identified primary afferents in trigeminal subnuclei principalis and oralis. J. Neurophysiol. 70: 1911-1936.

Jacquin M.F., Rhoades R.W. (1985) Effects of neonatal infraorbital lesions upon central trigeminal primary afferent projections in rat and hamster. J. Comp. Neurol. 235: 129-143.

Jacquin M.F., Semba K., Rhoades R.W., Egger M.D. (1982) Trigeminal primary afferents project bilaterally to dorsal horn and ipsilaterally to cerebellum, reticular formation, and cuneate, solitary, supratrigeminal and vagal nuclei. Brain Res. 246: 285-291.

Jacquin M.F., Woerner D., Szczepanik A.M., Riecker V., Mooney R.D., Rhoades R.W. (1986b) Structure-function relationships in rat brainstem subnucleus interpolaris. I. Vibrissa primary afferents J. Comp. Neurol. 243: 266-279.

Killackey, H.P (1973) Anatomical evidence for cortical subdivisions based on vertically discrete thalamic projections from the ventral posterior nucleus to cortical barrels in the rat. Brain Res. 51: 326-331.

Killackey G.P., Belford G.R., Ryugo R., Ryugo D.K. (1976) Anomalous organization of the thalamocortical projections consequent to vibrissae removal in the newborn rat and mouse. Brain Res. 104: 309-315.

Ma P.M., Woolsey T.A. (1984) Cytoarchitectonic correlates of the vibrissae in medullary trigeminal complex of the mouse. Brain Res. 306: 374-379.

Marfurt C.F., D.M. Rajchert (1991) Trigeminal primary afferent projections to "non-trigeminal" areas of the rat central nervous system. J. Comp. Neurol. 303: 489-511.

Melzer P., Van der Loos H., Dorfl J., Welker E., Robert P., Emery D., Berrini J.-C. (1985) A magnetic device to stimulate selected whiskers of freely moving or restrained small rodents: its application in a deoxyglucose study. Brain Res. 348: 229-240.

Melzer P., Welker E., Dorfl J., Van der Loos H. (1994) maturation of the neuronal metabolic response to vibrissa stimulation in the developing whisker to barrel pathway of the mouse. Devp. Brain Res. 77: 227-250.

Pfaller K, Arvidsson J. (1988) Central distribution of trigeminal and upper cervical primary afferents in the rat studied by anterograde transport of horseradish peroxidase conjugated to wheat germ agglutinin. J. Comp. Neurol. 268: 91-108.

Rhoades R.W., Chiaia N.L., Macdonald G.J., Jacquin M.F. (1989) Effect of fetal infraorbital nerve transection upon trigeminal primary afferent projections in the rat. J. Comp. Neurol. 287: 82-97.

Robertson B., Arvidsson J. (1985) Transganglionic transport of wheat germ agglutinin-HRP and choleragenoid-HRP in rat trigeminal primary sensory neurons. Brain Res. 348: 44-51.

Takemura M., Sugimoto T., Shigenaga Y. (1991) Difference in central projection of primary afferents innervating facial and intraoral structures in the rat. Exp. Neurol. 111: 324-331.

Van der Loos, H. (1976) Barreloids in mouse somatosensory thalamus. Neurosci. Lett. 2: 1-6.

Van der Loos, H., Woolsey T.A. (1973) Somato-sensory cortex: structural alterations following early injury to sense organs. Science 179: 395-398.

Woolsey T.A., Anderson J.R., Wann J.R., Stanfield B.B. (1979) Effects of early vibrissae damage on neurons in the ventrobasal (VB) thalamus of the mouse. J. Comp. Neurol. 184: 363-380.

Woolsey T.A., Van der Loos H. (1970) The structural organization of layer IV in the somatosensory region (SI) of the mouse cerebral cortex. Brain Res. 17: 205-242.

Received 20 April 1995, accepted 21 May 1995